Hindawi
Advances in Materials Science and Engineering
Volume 2018, Article ID 3637873, 10 pages
https://doi.org/10.1155/2018/3637873

Research Article

High-Temperature Superconducting Cable Design Based on Individual Insulated Conductors

Peter Cheetham,[1] Jose Viquez,[1] WooJin Kim,[1] Lukas Graber,[2] Chul H. Kim,[1] and Sastry V. Pamidi[1,3]

[1]*Center for Advanced Power Systems, Florida State University, 2000 Levy Avenue, Tallahassee, Florida 32310, USA*
[2]*School of Electrical and Computing Engineering, Georgia Institute of Technology, 777 Atlantic Drive NW, Atlanta, Georgia 30332, USA*
[3]*Department of Electrical and Computer Engineering, FAMU-FSU College of Engineering, 2525 Pottsdamer Street, Tallahassee, Florida 32310, USA*

Correspondence should be addressed to Peter Cheetham; cheetham@caps.fsu.edu

Received 1 May 2018; Revised 10 August 2018; Accepted 9 October 2018; Published 1 November 2018

Academic Editor: Charles C. Sorrell

The idea of insulating individual high-temperature superconducting (HTS) tapes was explored as a dielectric design to reduce the risk and complexity of HTS cable manufacturing. Applying insulation on individual HTS tapes is amenable to continuous manufacturing processes and opens up material choices for the insulation. In this study, heat shrink insulation was selected as the material choice for exploring the possibility of this design philosophy because of its commercial availability in multiple thicknesses. A systematic set of selection criteria was developed for the selection of appropriate heat shrink for given HTS tape dimensions. The cryogenic dielectric characteristics of insulated HTS tapes were evaluated both in liquid nitrogen and gaseous helium environments at 77 K. Dielectric characteristics of tapes with a single layer of thicker insulation were compared with those insulated using multiple layers of thinner insulation to evaluate the relative merits of each method. Several model power cables were fabricated using the PET insulated tapes, and their dielectric behavior was evaluated at 77 K in gaseous helium environment. The results suggest that the explored method is useful for HTS power cables operating at low voltages (<1,000 V) primarily due to the limitation on achieving thick insulation with high quality using heat shrink tubing. The suitable processes of insulating longer lengths of samples with additional dielectric benefits are discussed.

1. Introduction

The design, fabrication, and installation of high-temperature superconducting (HTS) power devices is a complex process [1]. A single handling error during the fabrication and insulation stages could cause irreversible damage to the cable. In some instances, the damage to the HTS power cable may not be discovered until it is installed and commissioned. Currently, the high cost of HTS conductor, lack of choice in dielectric insulation materials and application processes, and large scale cryogenic cooling systems with low maintenance are hindering the widespread implementation for HTS power devices for commercial applications. HTS power devices that have been incorporated into power grids have typically been demonstration projects that have been subsidized by federal and local governments [2]. Successful reduction of complexity and risks in HTS technology is expected to increase the appeal and acceptance of HTS power devices for a variety of applications including the electric power grid, data centers, electric ships, electric airplanes, and feeder cables for high energy physics. Cost-effective HTS devices will allow these applications to exploit the significant increase in their power density and the associated reduction in footprint as well as their increased efficiency. The operating voltages of the applications listed above are in the low voltage to medium voltage range. HTS

technology is particularly beneficial to low voltage and high current applications such as electric aircraft. Low voltage HTS cables in power distribution systems for train networks eliminate the need for multiple substations because the voltage drop in HTS cables is significantly smaller compared to the conventional technology [3]. One of the focus areas in the superconducting power applications research at Florida State University's Center for Advanced Power Systems (FSU-CAPS) and at Georgia Tech's Plasma and Dielectrics Laboratory is the development of novel dielectric insulation materials and designs.

The design of HTS power cables comes with some challenging design constraints that do not exist in room temperature power cables. These constraints include the need for cryogenic operating environment and the associated mechanical stresses caused by the mismatch among the coefficients of thermal expansion (CTE) of various materials used in HTS power cables. Typically, a cold dielectric design is employed for HTS cables to electrically insulate the HTS power cable from the grounded cryostat [4]. In this design, the insulation operates at cryogenic temperatures. Traditional electrical insulation designs of extruding insulation over the entire cable are not compatible with a cryogenic environment due to the large difference in the CTE values of the insulation material and the metallic and ceramic components of the HTS cables [5, 6]. This mismatch in CTE causes significant mechanical stresses on the HTS tapes and the insulation layers leading to potential degradation of the superconducting properties. Furthermore, the mechanical stresses cause delamination and voids in the insulation material affecting the dielectric integrity of the cable system [5]. To circumvent the mechanical issues, HTS cables typically use lapped tape of CryoFlex^{TM} or polypropylene laminated paper (PPLP) as the insulation [7–10]. While the lapped tape insulation provides insulation for HTS cables, this method does not lend itself to quality control tests in the factory because the dielectric integrity can only be tested in the completely installed cable after cooling it to the cryogenic operating temperatures. The inability to test the dielectric integrity of HTS cables at the manufacturing facility transfers the risk to the cable operators, and any defect noticed after the installation and cool down is costly and it is more costly to correct.

In an attempt to identify alternative dielectric materials and designs for HTS power cables that would reduce the complexity and enable quality control tests before the cable is fabricated and installed, a study has been undertaken on exploring insulation of individual HTS tapes before using them in cable manufacturing. The mechanical stresses from applying the insulation to individual HTS tapes instead of the manufactured cable are lower, which lowers the risk of damaging the insulation and/or superconducting layer. A typical HTS power cable consists of between 10–30 HTS tapes per phase, depending on the current rating. There is no difference in insulating individual tapes or insulating entire cable since insulation of individual tapes does not affect the operational rating of the cable (Figure 1). The main motivation for insulating each tape individually by heat shrink was to reduce the complexity of the cable fabrication process. Insulated HTS tapes are beneficial to large scale manufacturing unlike the traditionally used lapped tape design as the dielectric layer can be applied using traditional processes such as extrusion and coating. Such individually insulated HTS tapes can be spooled and processed in (modified) cable winding machines. Large availability of insulated HTS conductors saves the time, cost, and risk of damage in the cable manufacturing process. More streamlined and efficient fabrication processes can help to increase the desirability of HTS cables as well as accelerate the commercial deployment of HTS cables in the low-medium voltage range. More importantly, the quality of the insulation process and the dielectric integrity of the cables can be tested at room temperature on the tape spools.

Another potential benefit of using insulated HTS tapes is to increase the partial discharge inception voltage (PDIV) of HTS cables. HTS cables are operated below the PDIV to reduce the possibility of partial discharge processes degrading the dielectric material and eventually compromising the dielectric integrity that might lead to a failure of the HTS cable. For a lapped tape insulated HTS cable, partial discharge occurs in the butt gaps between the lapped tape insulation which are made to allow for mechanical flexibility of the HTS cable. Individually insulated HTS tapes do not contain butt gaps in the dielectric design. The PDIV is a function of the dielectric strength of the cryogen used. Published studies on lapped tape insulated HTS cables demonstrated that using LN_2 as the cryogen has allowed cables with voltage ratings in excess of 100 kV. When the same cable design is utilized for gaseous helium (GHe) cooled cables, a significantly lower voltage suitability at <10 kV was noticed. As our research focuses on GHe cooled HTS technology [1], it is of importance to consider the implication of the cryogen's dielectric strength on the overall voltage rating.

There are various methods available to apply insulation onto the HTS tapes including extrusion, dip coating, and heat shrink. Heat shrink was selected for this study as it allowed an easy method to ensure a uniform insulation with varying thickness. Heat shrink has been reported as turn-to-turn insulation for HTS magnet coil applications [11]. As the heat shrink is not directly bonded onto the HTS tape, it was not expected to cause any significant mechanical stress onto HTS tape. While the heat shrink does not have a direct bond to the HTS tape, there is the potential of air pockets generated in the process, but the size of these voids would be significantly smaller than the butt gaps in the lapped tape design. Extrusion or dip coating will further reduce the size of voids but come with an increased shear stress at the interface when cooled to cryogenic temperature. A good strategy will be to keep the insulation thickness low.

The following sections provide details on the benefits from individually insulated in fabricating HTS cables. This paper also describes the selection criteria implemented for heat shrink materials, heat shrink properties, and dielectric measurements in LN_2 on HTS tapes insulated with heat shrink. The fabrication and dielectric characterization of 1 m long model cables insulated with commercially available polyethylene terephthalate (PET) heat shrink are described.

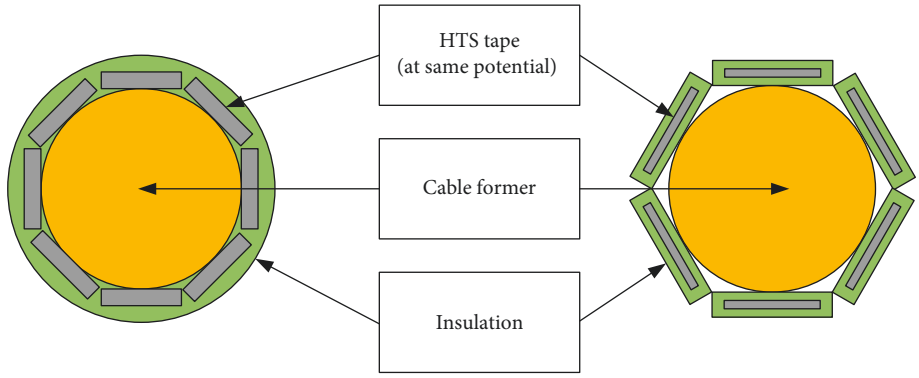

Figure 1: Lapped tape insulated HTS cable (left) and individually insulated HTS tape cable configuration (right) (note: not to scale and a typical HTS cable would consist of more HTS tapes).

The overarching goal of this research was to develop a new dielectric design concept.

2. Insulation for Individual Conductors

Before considering the insulation material to be applied to the HTS tape, it is first necessary to understand the manufacturing technique used to produce the HTS tape. The type of HTS tape selected can influence the selection criteria of the insulation material. HTS tapes can be manufactured using ion-beam assisted deposition (IBAD), rolling assisted biaxially textured substrates (RABiTS), and inclined-substrate deposition (ISD) [12]. Each of these manufacturing techniques uses different fabrication principles to develop the HTS tape and therefore the HTS tapes have different maximum temperatures limits and geometries. For example, HTS tape manufactured using the IBAD technique has a maximum operating temperature of 240°C whereas HTS manufactured using RABiTS has a maximum operating temperature of 175°C [REF].

Heat shrink was selected as the chosen method to provide insulation to HTS tapes in this study as many types of polymers are commercially available in heat shrink form. Also, it is simple to apply at short lengths without expensive equipment. To identify the potential insulation materials suitable for HTS tapes and cables, a selection criteria matrix was established. In developing the criteria, several electrical and mechanical characteristics were considered, including shrink temperature, dielectric strength, relative permittivity, volume resistivity, CTE, and thermal conductivity. A comparison of these properties was performed for polytetrafluoroethylene (PTFE), fluorinated ethylene propylene (FEP), polyether ether ketone (PEEK), and polyethylene terephthalate (PET), with the results shown in Table 1. The data from Table 1 were obtained from commercial suppliers of heat shrink [13, 14].

Table 1 indicates that PTFE, FEP, and PEEK have a shrink temperature greater than 175°C, the maximum allowable for most bonded HTS tapes. Exceeding this temperature could cause the HTS tape to delaminate and damage the superconducting layer. Therefore, only the PET heat shrink was selected for further investigations.

PET heat shrink is commercially available in various diameters and wall thicknesses. After consultations with a supplier, it was discovered that the best results for a uniform finish are obtained by using a heat shrink circumference that is a maximum of 15% larger than the HTS tape circumference resulting in a shrink ratio of marginally less than 15%. Comparing the circumference of the HTS tape (10.3 mm) to the circumference of the heat shrink tube, it was determined that a heat shrink must have a maximum expanded internal diameter of 3.85 mm. A heat shrink with expanded internal diameter of 3.6 mm was chosen as it allowed for a shrink rate of 7.8% and also it has variety of wall thicknesses available in 6.35, 12.7, 19.1, 25.4, 50.8, and 76.2 μm, increasing linearly from 0.5 to 6 times of 12.7 μm.

The primary reason for using several wall thicknesses is to establish a relationship between the thickness of the insulation and the breakdown voltage. Another reason to examine several wall thicknesses was to determine if multiple layers of a thinner heat shrink are dielectrically and mechanically equivalent to a single layer of a thicker heat shrink with the same total thickness. This was seen as important as the largest wall thickness commercially available was only 76.2 μm (before shrinking) which by itself would considerably limit the suitable operation voltage.

To obtain initial data, experiments were undertaken on individually insulated HTS tapes in LN_2. The two experiments which were performed in LN_2 were to examine the critical current of heat shrink insulated HTS tapes and to evaluate the dielectric strength of the various wall thickness of the heat shrinks discussed above. LN_2 was selected for quick evaluation of many samples to build a set of statistically relevant data. Subsequently, electrical breakdown experiments were conducted in gaseous helium (GHe). Second generation (2G) HTS tapes were used in the experiments.

3. Critical Current Measurements on Insulated HTS Tapes in LN_2

3.1. Sample Preparation. Critical current measurements were performed on HTS tapes insulated with the 76.2 μm

Table 1: Important properties for selected heat shrink materials.

Material	Shrink temp (°C)	Dielectric strength (kV/mm)	Relative permittivity	CTE (μm/m-K)	Thermal conductivity (W/m-K)
PTFE	346–354	7–24	2.1	126–180	0.17–0.30
FEP	204–216	20–79	2.0–2.1	100–135	0.19–0.25
PEEK	330–360	20	2.2–2.8	47	0.25
PET	85–190	17	3.3	59	0.15
Ideal heat shrink	<175	As high as possible	1	10–20	As high as possible

thick heat shrink. Measurements were performed on HTS tapes with 1, 2, and 3 layers of the 76.2 μm heat shrink.

Substantial effort went into the development of a reliable and reproducible method of applying heat shrink to HTS tapes without introducing air pockets or wrinkles. A convection oven was used in the preparation of the insulated tape samples to provide the entire tape specimen with uniform temperature. Samples were placed in the convection oven for 5 minutes at 100°C, which was sufficient time for heat shrink tube to be shrunk. It was found that fixing the heat shrink in place at both ends of the HTS tape prevented the heat shrink from being shrunk longitudinally, which otherwise can result in wrinkles in the material.

3.2. Experimental Setup for Critical Current Measurements. Figure 2 depicts the experimental setup for measuring critical current of the tapes, which depicts the HTS tape soldered onto two current leads. Voltage taps were soldered 15 cm apart on the HTS tape to measure the transition from superconducting to normal state. Soldering the voltage taps onto the HTS tape ensured the same gap distance for all of the measurements. The critical current measurements were completed by submerging the whole experiment setup in a bath of LN_2, and a sufficient wait time was included before the measurements of critical current. Critical current of the tapes is defined using the standard criteria of 1 μV/cm. A ramp generator was used to control the ramp rate of the applied current during the critical current measurement. The measurements tracked the variation of critical current of the tapes.

Critical current of the 2G HTS was measured on a procured and uninsulated tape to get a baseline reading for comparison. The HTS tape was then removed from the experiment setup and a 14 cm length of the 76.2 μm heat shrink was applied to the HTS tape in between the potential taps using the method which was described above. The HTS tape was then resoldered onto the experimental setup, and the critical current was measured. This procedure was then repeated with a 2nd and 3rd layers of the 76.2 μm heat shrink being applied to the HTS tape.

3.3. Results. The results of the critical current measurements of the HTS tape with various layers of the 76.2 μm heat shrinks can be seen in Figure 3.

The data shown in Figure 3 demonstrate that the application of the heat shrink onto the HTS tape does not result in degradation of the critical current. There is no excessive mechanical force applied to the HTS tape by the heat shrink when it is cooled to cryogenic temperatures. Repeated handling of the insulated HTS tape including the soldering and unsoldering from the experimental setup also demonstrates the ruggedness of the individually insulated HTS tape.

4. Dielectric Measurements on Insulated HTS Tapes in LN_2

4.1. Sample Preparation. Heat shrinks with an inner diameter of 3.6 mm and wall thicknesses of 12.7, 25.4, 50.8, and 76.2 μm were selected for measurements as 1, 2, 4, and 6 times of thinnest shrink tube (noted as 1x, 2x, 4x, and 6x). Samples were prepared with 1, 2, and 3 layers of heat shrink with each thickness. In total 12 types of samples were prepared with each sample consisting of 8 cm of heat shrink tube in length onto a 15 cm long HTS tape with the same dimensions of the HTS tape previously described. The 8 cm insulated section of the samples was long enough to perform three breakdown voltage measurements on each sample by moving it to a section of unused insulation surface after each measurement.

4.2. Experimental Setup for Dielectric Measurements. To characterize the dielectric properties of heat shrink with various wall thicknesses, AC breakdown measurements were performed at 77 K in a bath of LN_2. These measurements were performed by placing the insulated tape sample between two 25 mm diameter uniform field electrodes. The electrodes were designed with the geometry similar to Bruce profile [15]. Sufficient cooling time was allowed for the samples to reach a uniform temperature of 77 K before the measurements were performed. The electrodes were both connected to the high-voltage power supply. The sample was kept at ground potential. The pair of electrodes creates an electric field between the electrode surface and the tape. The breakdown could occur on either side of the insulated tape sample since the electric field profile is symmetric. A ground wire was soldered onto the bare section of the sample as shown in the experiment setup depicted in Figure 4.

The voltage supplied to the electrodes was manually increased in steps of 300–500 V until breakdown occurred. Once breakdown occurred, the sample was examined and repositioned to allow for another breakdown measurement of the next unused section.

4.3. Results. The results of the breakdown voltage measurements on tape samples in LN_2 are shown in Figure 5 for four heat shrink materials for up to three layers.

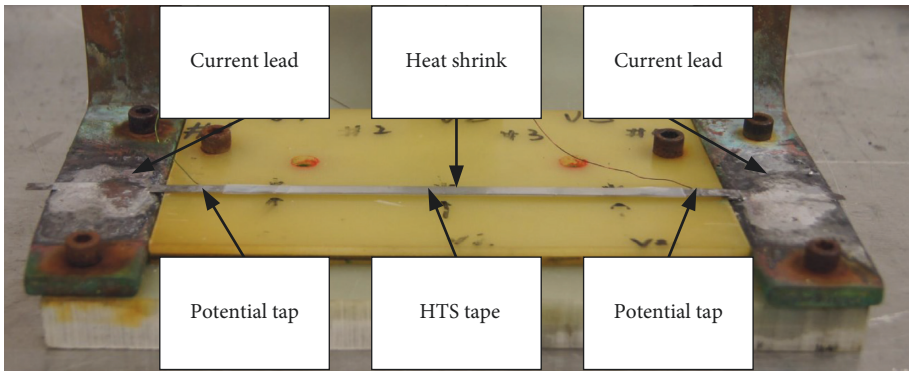

Figure 2: Experiment setup to measure critical current of the HTS tape.

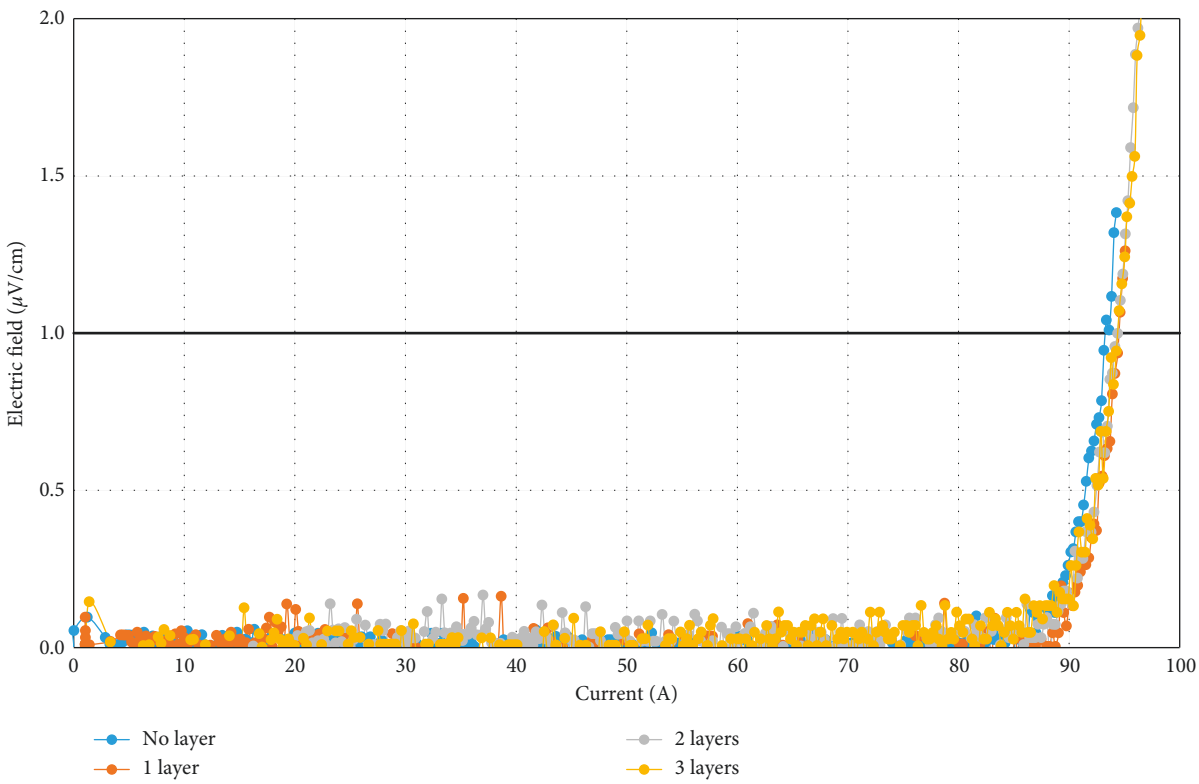

Figure 3: Current-voltage traces used to evaluate critical current of HTS tape insulated with 76.2 μm heat shrink.

Figure 5 shows that breakdown voltage of the tapes with heat shrink is a function of the number of layers. The breakdown voltage increased with the heat shrink thickness. However, as can be seen from the data in Figure 5, the relationship between the breakdown voltage and the insulation thickness is not linear. From the comparison of the breakdown voltages of the 2x and 4x samples, use of heat shrink that is twice as thick did not result in breakdown voltages twice as large. Figure 5 also shows that multiple layers of a thinner material (e.g., 2 layers of 2x heat shrink) had higher breakdown voltages compared to fewer layers of a thicker heat shrink (e.g., 1 layer of 4x heat shrink).

Visual inspection of the spots of breakdown piercing locations allowed two important observations: the first observation was that the breakdown hole typically occurred at the center of the HTS tape. This suggests that the heat shrink insulation is thicker on the edges, where the electric field is even higher. The second observation was that the multiple layer samples showed evidence of electrical treeing, which is a sign of partial discharge occurring before the actual breakdown happened as seen by the streaking marks (Figure 6).

Figure 6 suggests that voids were present between the layers of the heat shrink. The occurrence of voids of this magnitude is not expected if a thicker heat shrink was used or an alternative method to apply the insulation was adopted. Therefore, a single layer of heat shrink with wall thickness of 76.2 μm (6x) is preferred from a dielectric point

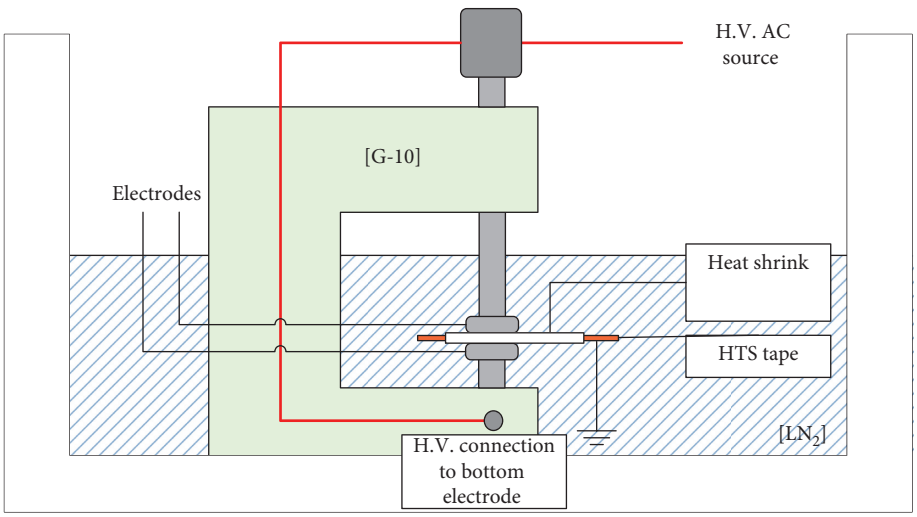

Figure 4: A schematic of the experimental setup used for breakdown voltage measurements on insulated tape in LN_2.

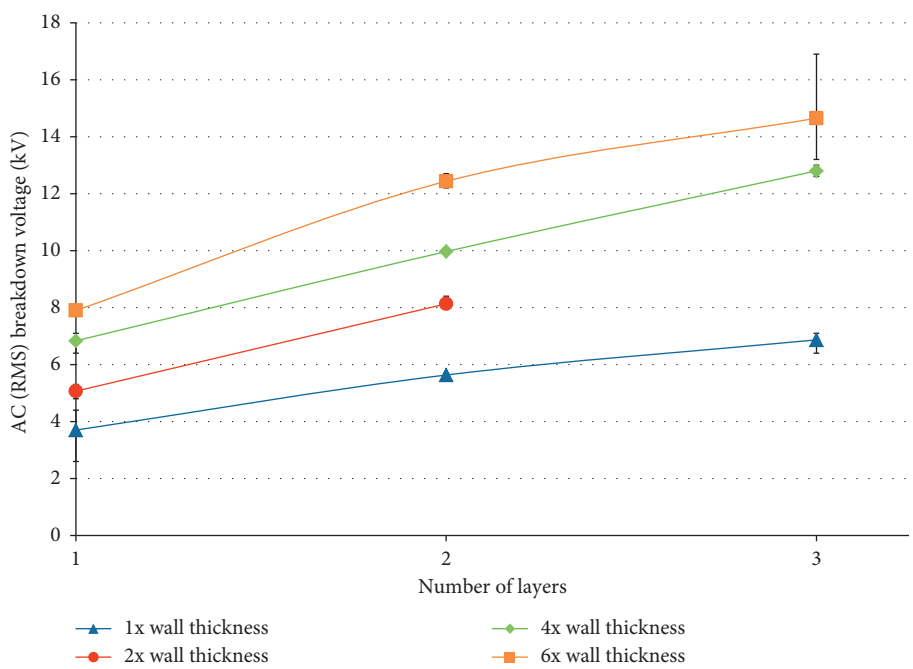

Figure 5: AC (RMS) breakdown voltages of small scale samples in LN_2.

of view and needed to be further examined for the development of 1 m HTS model power cables.

5. Heat Shrink Model Cables

5.1. Background. Two slightly different HTS tapes were used to make two model cables. Tape 1 had a width of 4.4 mm, a thickness of 0.4 mm, and a circumference of 9.6 mm. Tape 2 had a width of 4.0 mm, a thickness of 0.2 mm, and a circumference of 8.4 mm. The circumference of the two new HTS tapes was slightly smaller than the previous HTS tape used in short samples discussed earlier. In keeping with the recommendations made from the supplier, heat shrinks with <15% shrink ratio were initially selected for both materials. However, there was excessive friction between the heat shrink and HTS tapes when applying the heat shrink on 1 m samples. This complicated the process of applying heat shrink and increased the possibility of damaging the HTS tape or the heat shrink. It was therefore decided to use the next larger available inner diameter of the heat shrink tubing. Tape 1 used a 4.06 mm inner diameter heat shrink and Tape 2 used a 3.56 mm heat shrink. The shrink ratio for both combinations of HTS tape and heat shrink resulted in a shrink ratio of 25%. As the shrink ratio exceeded the recommended 15% shrink ratio, it was decided to verify the electrical properties of these heat shrinks before beginning fabrication of the model cables. AC and DC breakdown measurements were performed on both types of HTS tape as

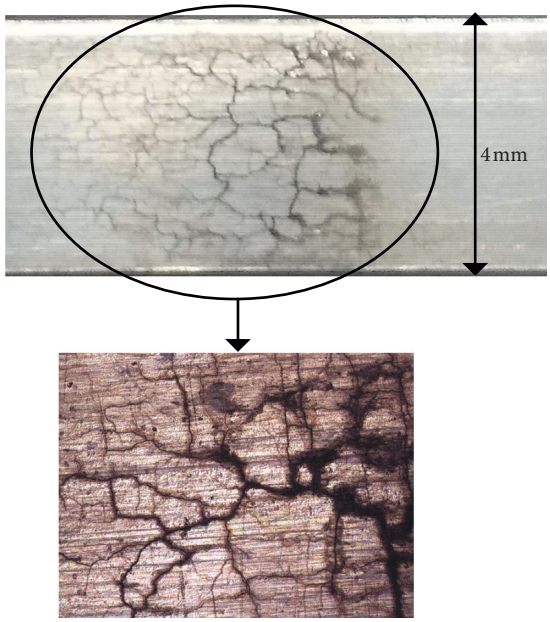

Figure 6: Optical micrograph of the damage after an AC breakdown event of a sample with multiple layered heat shrink. Optical micrograph shows the damage to both the heat shrink and metallic surface of the HTS tape.

well as partial discharge (PD) measurements. The measurements were performed using the same method (outlined previously). The results of these measurements are summarized below in Table 2.

Table 2 shows that the AC and DC breakdown voltages are similar for both HTS tapes. This suggests that the breakdown voltage is dependent on the wall thickness of the heat shrink and not a function of the geometry of the HTS tape. The PDIV values in Table 2 are based on the definition of the voltage where the apparent discharge exceeded 10 pC. For both HTS tapes, the apparent charge sharply rose in excess of 10 pC when ramping up the voltage. The occurrence of PD before breakdown suggests that there are only small voids present in between the HTS tape and heat shrink since voids of significant size inside the heat shrink material are unlikely.

5.2. Fabrication of Model Cables Using HTS Tapes with Heat Shrink. Four model cables were fabricated; two for each of the HTS tape type. For both cables, a pitch angle of 25° was selected, and a solid copper former with an outer diameter of 15.9 mm was used. This resulted in a cable with one layer of 10 insulated tapes for the 4.4 mm HTS tape and 11 tapes for the 4 mm HTS tape. A single layer design was selected as it allowed for the dielectric properties of the heat shrink to be characterized without having to use long lengths of HTS tape.

Hot air from a heat gun was applied to shrink the heat shrink onto the HTS tapes since the sample was too long to fit into the convection oven. The hot air was directed along and around the tape to ensure a smooth finish, which was free of any visible voids. Helically wrapping the heat shrink-insulated HTS tapes on the copper former was completed without any damage to the HTS tapes. This demonstrated that the bending properties of the 6x heat shrink are suitable for fabricating the cables.

To ensure that the HTS tapes are at the same voltage potential as the cable former, part of the heat shrink was removed from both ends of the HTS tapes. Both uninsulated end sections of the HTS tapes were soldered onto the copper former. Stress cones were added onto each end of the cables using a PET sheet with 76.2 μm thickness. A semiconductive carbon layer and a copper shield layer were then added to the cable. Butt gaps were introduced to both the semiconductive and the shield layers to ensure no excessive mechanical stress was applied to the heat shrink-insulated HTS tapes during the cooling cycle. The cable layout including stress cone can be seen in Figure 7.

5.3. Experimental Setup for Dielectric Measurements on Model Cables. To characterize the dielectric properties of the heat shrink-insulated HTS cables, AC breakdown and PD measurements were conducted in a high purity GHe environment at 77 K. The model cables were installed within a pressure vessel. The cable was connected to a high voltage bushing installed on the top plate of the pressures vessel. A 25 mm stress sphere was connected to the bottom end of the cable to minimize the electric field at the cable termination. A ground wire was attached to the shield layer of the cable and connected to the inside of the pressure vessel, which was at ground potential. Figure 8 shows a schematic of the experimental arrangement.

Care was taken to minimize impurities in the gas environment since they could freeze in small cavities inside the cable insulation. To ensure the high purity of the setup, several cycles of pumping and purging were carried out. Initially, a dry scroll pump was connected to the pressure vessel to reach a vacuum of at least 1 Pa. The pressure vessel was then flushed with 2.0 MPa of N_2 gas at room temperature. The dry scroll pump was then reconnected and allowed to pump for a minimum of an hour to ensure a vacuum of 1 Pa or better. Subsequently, the pressure vessel was flushed twice with industrial grade GHe (99.8% purity) at 2.0 MPa at room temperature, following the same procedure described in between each flushing phase. Finally, the pressure vessel was evacuated down to 10^{-2} Pa using a turbo molecular pump and then filled with 2.0 MPa of research grade GHe (99.9999% purity) at room temperature. At this point, the environment within the pressure vessel was determined to be of sufficiently high purity.

After establishing a high purity gas environment, the pressure vessel was immersed in LN_2 and pressurized with 2.0 MPa of research grade GHe at 77 K. Adequate time was given to allow the experiment inside the vessel to reach thermal equilibrium at 77 K as ensured by the constant pressure in the vessel before conducting the measurements.

AC partial discharge measurements were performed on the 1 m model cables by connecting a 100 kV, 7.5 kVA AC transformer to the high voltage bushing mounted on the pressure vessel. A high-voltage capacitor was used to record

Table 2: Electrical properties of small scale samples in LN_2.

HTS tape	Average AC breakdown voltage (kV)	Average DC breakdown voltage (kV)	Average PDIV (kV)
4.4 mm	7.6	15.1	5.5
4.0 mm	7.6	14.1	5.2

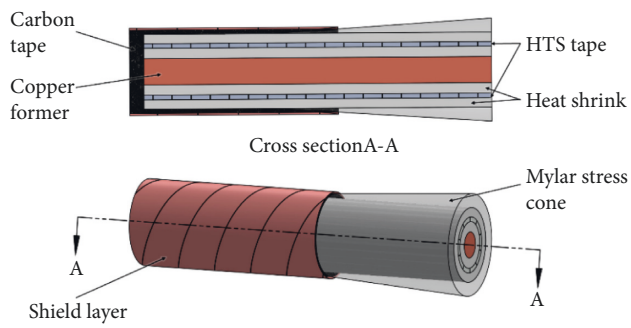

Figure 7: A sketch of one of the cables built for measuring the model cable with heat shrink-insulated tapes (not to scale and pitch angle exaggerated).

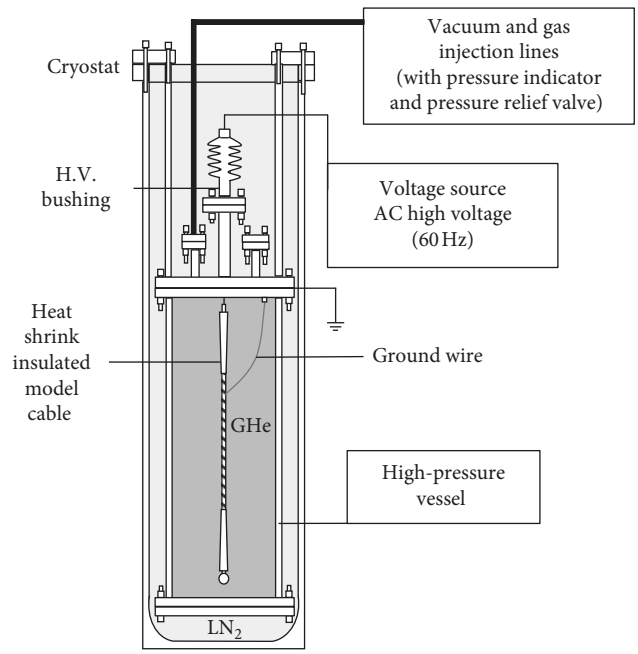

Figure 8: A schematic of the experimental setup used for breakdown voltage measurements on the model cables in 2.0 MPa GHe at 77 K.

the partial discharge activity of the cable. The voltage was increased in steps of approximately 300–500 V while the apparent charge was recorded at each voltage step.

5.4. Results. AC partial discharge measurements were completed on the four model cables at 2.0 MPa in GHe at 77 K. Unfortunately, breakdown of the cable insulation occurred suddenly without the partial discharge measurements giving any indication of insulation deterioration. Therefore, the authors were unable to perform partial discharge measurements at additional pressure ranges. A summary of the AC breakdown voltages for the heat shrink model cables can be seen in Table 3.

On completion of the AC breakdown measurement, the cables were removed from the pressure vessel and dissected. Dissection of the model cables showed that breakdown had occurred near the center part of the cable far from both stress cones. For the four model cables, the breakdown had occurred at random locations on the HTS tape including the edge, center, and in between two HTS tapes.

6. Discussion

Table 3 shows that the AC breakdown voltages of the model cables are significantly lower than the AC breakdown voltages of the individual HTS tape samples found in Table 2. This discrepancy might be due to different electric field stress caused by variations in the experimental setup and the fabrication process for individual HTS tapes and model cables.

Firstly, the two experiments resulted in different electric field stress: the Breakdown measurements on individual HTS tapes were performed in between two electrodes, which ensured a uniform electric field. However, the electric field experienced by the HTS tapes on the model cables is similar to a coaxial electric field. Further distortion originates in neighboring tapes. The breakdown of a dielectric material is highly governed by local electric field. Finite element models (FEM) to observe the electric fields for both cases were not developed because thickness and shape of the heat shrink tapes cannot be accurately modeled after being applied to the HTS tape. As mentioned previously, the location of the AC breakdown measurements on the individual HTS tapes suggested that the heat shrink insulation is thicker on the edges. The details of geometry of heat shrink on HTS tapes to develop FEM model is beyond the scope of this research.

Secondly, breakdown voltage of the heat shrink may have been influenced by the cryogen used. Both experiments were performed at 77 K; however, LN_2 was used for the individual HTS tapes, and GHe was used for the model cable. From completing the individual HTS tape measurement, partial discharge was recorded, which suggests there were voids between the heat shrink and HTS tape. These voids would have been filled with the cryogen during the experiment. The relative permittivity of LN_2 (1.45) is a closer match to PET (3.3) than that of GHe (1.0). The dielectric strength of LN_2 is also superior compared to GHe. Therefore, the LN_2 may have added additional dielectric strength to the heat shrink, while reducing the electric field enhancement in the voids, which resulted in a higher AC breakdown voltage when compared to GHe.

Thirdly, an additional factor lies in the difference in the fabrication processes for individual samples and model

Table 3: AC breakdown measurements of heat shrink model cables.

HTS tape	Cable 1 AC breakdown voltage (kV)	Cable 2 AC breakdown voltage (kV)
4.4 mm	1.8	1.8
4.0 mm	1.0	1.4

cables. For the individual HTS tape samples, a convention oven was used to ensure a uniform temperature was applied to the heat shrink while shrinking onto the HTS tape. For the model cable, hot air from a heat gun shrunk the heat shrink tube onto the HTS tape. This process to apply the heat shrink onto the HTS tape does not completely guarantee a uniform temperature field along the length of the sample, which may have increased the possibility of introducing small voids. Once the HTS tapes for the model cable were prepared, they were wrapped helically onto a former and had a semiconductive layer, shield layer, and stress cones built on top of them. This additional extra handling of the heat shrink-insulated HTS tapes increased the probability of imperfections being introduced to the heat shrink surface, which may have reduced the dielectric strength of the cable.

Fourthly, the size of the samples measured also has to be taken into consideration. For the individual HTS tape sample, the electric field applied to the HTS tape was essentially the diameter of the electrodes (25 mm). For the model cables, there was an excess of 10 m of heat shrink-insulated HTS tape on each cable. Having an overall larger area covered by heat shrink insulation, the probability of introducing defects in the insulation in the form of voids or physical damage due to handling and stress is greater. Also, the model cable design effectively had multiple heat shrink-insulated HTS tapes being tested at the same time. As the cable was being cooled to cryogenic temperatures, friction between two tapes might damage the insulation in contact. For one of the model cables breakdown was observed between two HTS tapes, which may have been a result of excessive friction.

Finally, the most noteworthy limiting factor for the AC breakdown strength of the model cables measured was the wall thickness of the heat shrink itself. The dielectric strength of PET was reported in Table 1 as 17 kV/mm. Only a single layer of heat shrink with wall thickness of 76.2 μm was used as the entire insulation of the cable. While the effective thickness of the heat shrink after shrinking is not known, an AC breakdown voltage of 1.2 kV is within the expected voltage range for PET with this thickness. If a PET heat shrink with a thicker wall thickness was used, a higher AC breakdown voltage should be observed. However, increasing wall thickness of the heat shrink requires in-depth consideration since excessive mechanical forces on the HTS tape and poor heat transfer will be also accompanied.

This paper demonstrates how an HTS cable can be fabricated by individually insulating each HTS tape. The results of the model cable suggest that greater care needs to be taken in the preparation and fabrication of the heat shrink-insulated HTS cables. Ensuring a uniform thickness of the heat shrink is of upmost importance to allow for the highest possible voltage rating of the HTS cable. A carefully extruded layer of PET is expected to result in higher dielectric strength, which would qualify such an insulation system for low voltage (<1,000 V) or potentially medium voltage (>1 kV) operation.

7. Conclusion

A new dielectric design of HTS cables involving individual insulated HTS tapes insulated with polyethylene terephthalate (PET) heat shrink is described. The new dielectric design with individual insulated tapes lends itself for continuous manufacturing process using several of the coating techniques available. For this project, heat shrink tubing was chosen as the dielectric system in lieu of an extruded or coated layer. A systematic sizing criterion for selecting the appropriate heat shrink was developed. The dielectric characteristics of insulated HTS tapes as well as the 1 m long model cables were measured at 77 K in liquid nitrogen and gaseous helium environments, respectively. A comparison of the dielectric characteristics of tapes with single layer of thicker insulation with multiple layers of thinner insulation showed similar breakdown strengths. However, a single thicker layer is better for preventing trapped air pockets between the layers that could cause partial discharge at lower voltages. The initial assumption that multiple layers of thinner heat shrink result in improved bending properties compared to a single thicker heat shrink could not be confirmed. It was observed during the fabrication of the model cables that tapes with a thicker heat shrink could be helically wrapped onto the former without damaging the HTS tapes and are therefore preferred in the design of HTS cables. The new dielectric design allows qualification testing of insulation system of the cable prior to installation. Furthermore, the dielectric design reduces the risk for damaging the HTS cable while handling and installing.

Data Availability

The data used to support the findings of this study are available from the corresponding author upon request.

Conflicts of Interest

The authors declare that they have no conflicts of interest.

References

[1] S. Pamidi, C. H. Kim, and L. Graber, "High-temperature superconducting (HTS) power cables cooled by helium gas," in *Superconductors in the Power Grid: Materials and Applications*, pp. 225-260, Woodhead Publishing, Sawston, UK, 2015.

[2] J. A. Demko, I. Sauers, D. R. James et al., "Triaxial HTS cable for the AEP bixby project," *IEEE Transactions on Applied Superconductivity*, vol. 17, no. 2, pp. 2047–2050, 2007.

[3] M. Tomita, M. Muralidhar, Y. Fukumoto et al., "Design and development of superconducting DC cable for railway applications," *IEEE Transactions on Applied Superconductivity*, vol. 23, no. 3, article 3601504, 2013.

[4] J. A. Demko et al., "Cryostat vacuum thermal considerations for HTS power transmission cable systems," *IEEE Transactions on Appiled Superconductivity*, vol. 13, no. 2, pp. 1930–1933, 2003.

[5] M. Kosaki, "Research and development of electrical insulation of superconducting cables by extruded polymers," *IEEE Electrical Insulation Magazine*, vol. 12, no. 5, pp. 17–24, 1996.

[6] A. Morandi, "HTS dc transmission and distribution: concepts, applications and benefits," *Superconductor Science and Technology*, vol. 28, no. 12, article 123001, 2015.

[7] J. H. Lim, S. H. Sohn, H. S. Ryoo et al., "Performance test of 100 m HTS power cable system," *IEEE Transactions on Applied Superconductivity*, vol. 19, no. 3, pp. 1710–1713, 2009.

[8] J. P. Stovall, J. A. Demko, P. W. Fisher et al., "Installation and operation of the Southwire 30-meter high-temperature superconducting power cable," *IEEE Transactions on Applied Superconductivity*, vol. 11, no. 1, pp. 2467–2472, 2001.

[9] L. Graber, C. H. Kim, S. V Pamidi, and D. Knoll, "Dielectric design validation of a helium gas cooled superconducting dc power cable," in *Proceedings of 2014 IEEE Electrical Insulation Conference*, pp. 157–161, Philadelphia, PA, USA, June 2014.

[10] J. Gerhold and T. Tanaka, "Cryogenic electrical insulation of superconducting power transmission lines: transfer of experience learned from metal superconductors to high critical temperature superconductors," *Cryogenics (Guildf).,* vol. 38, no. 11, pp. 1173–1188, 1998.

[11] U. P. Trociewitz, M. Dalban-Canassy, M. Hannion et al., "35.4 T field generated using a layer-wound superconducting coil made of (RE)Ba 2 Cu 3 O 7−x (RE = rare earth) coated conductor," *Applied Physics Letters*, vol. 99, no. 20, article 202506, 2011.

[12] M. W. Rupich, "Second-generation (2G) coated high-temperature superconducting cables and wires for power grid applications," in *Superconductors in the Power Grid*, pp. 97–130, Elsevier, Amsterdam, Netherlands, 2015.

[13] Zeus, https://www.zeusinc.com/products/heat-shrinkable-tubing, 2018.

[14] Norsdon medical, https://www.nordsonmedical.com/Components-and-Technologies/Medical-Tubing/Heat-Shrink-Tubing/, 2018.

[15] H. Rodrigo, D. Kwag, L. Graber, B. Trociewitz, and S. Pamidi, "AC flashover voltages along epoxy surfaces in gaseous helium compared to liquid nitrogen and transformer oil," *IEEE Transactions on Applied Superconductivity*, vol. 24, no. 3, pp. 3–8, 2014.